Journal of Hazardous Materials 186 (2011) 458–465

Contents lists available at ScienceDirect

Journal of Hazardous Materials

journal homepage: www.elsevier.com/locate/jhazmat

Kinetics and thermodynamics of cadmium ion removal by adsorption onto nano zerovalent iron particles

Hardiljeet K. Boparai*, Meera Joseph, Denis M. O'Carroll

Department of Civil and Environmental Engineering, Faculty of Engineering, The University of Western Ontario, 1151 Richmond St. N, London, Ontario N6A 5B9, Canada

ARTICLE INFO

Article history:
Received 7 September 2010
Received in revised form 4 November 2010
Accepted 7 November 2010
Available online 18 November 2010

Keywords:
Cadmium
Nano
Zerovalent iron
Adsorption
Kinetics
Isotherm

ABSTRACT

Nano zerovalent iron (nZVI) is an effective adsorbent for removing various organic and inorganic contaminants. In this study, nZVI particles were used to investigate the removal of Cd^{2+} in the concentration range of 25–450 mg L^{-1}. The effect of temperature on kinetics and equilibrium of cadmium sorption on nZVI particles was thoroughly examined. Consistent with an endothermic reaction, an increase in the temperature resulted in increasing cadmium adsorption rate. The adsorption kinetics well fitted using a pseudo second-order kinetic model. The calculated activation energy for adsorption was 54.8 kJ mol^{-1}, indicating the adsorption process to be chemisorption. The intraparticle diffusion model described that the intraparticle diffusion was not the only rate-limiting step. The adsorption isotherm data could be well described by the Langmuir as well as Temkin equations. The maximum adsorption capacity of nZVI for Cd^{2+} was found to be 769.2 mg g^{-1} at 297 K. Thermodynamic parameters (i.e., change in the free energy (ΔG^o), the enthalpy (ΔH^o), and the entropy (ΔS^o)) were also evaluated. The overall adsorption process was endothermic and spontaneous in nature. EDX analysis indicated the presence of cadmium ions on the nZVI surface. These results suggest that nZVI could be employed as an efficient adsorbent for the removal of cadmium from contaminated water sources.

1. Introduction

Cadmium is a toxic heavy metal of significant environmental and occupational concern [1]. It has been released to the environment through the combustion of fossil fuels, metal production, application of phosphate fertilizers, electroplating, and the manufacturing of batteries, pigments, and screens [2–4]. This heavy metal has resulted in serious contamination of both soil and water. Cadmium (Cd) has been classified as a human carcinogen and teratogen impacting lungs, kidneys, liver and reproductive organs [1,5]. The World Health Organization (WHO) has set a maximum guideline concentration of 0.003 mg L^{-1} for Cd in drinking water [6]. Given pervasive cadmium contamination and the low drinking water guideline, there is considerable interest in the development of techniques to remove cadmium from contaminated water.

Adsorption has been developed as an efficient method for the removal of heavy metals from contaminated water and soil. A variety of adsorbents, including clays, zeolites, dried plant parts, agricultural waste biomass, biopolymers, metal oxides, microorganisms, sewage sludge, fly ash and activated carbon have been used for cadmium removal [2,7–20]. Nano zerovalent iron (nZVI), an emerging technology, is being used to successfully treat various metallic ions in aqueous solutions (e.g., Cr^{6+}, Cu^{2+}, Pb^{2+}, Ba^{2+}, As^{3+}, As^{5+}, and Co^{2+}) [21–25]. Nano iron particles are particularly attractive for remediation purposes due to their significant surface area to weight ratio leading to a greater density of reactive sites and heavy metal removal capacity [26,27]. Moreover, the magnetic properties of nano iron facilitate the rapid separation of nano iron from soil and water, via a magnetic field [28,29]. Heavy metals are either reduced at the nZVI surface (e.g., Cu^{2+}, Ag^{2+}) or directly adsorbed to the nZVI surface where they are rendered immobile (e.g., Zn^{2+}, Cd^{2+}). The controlling mechanism is a function of the standard redox potential of the contaminant metal. The standard redox potential of Cd^{2+} (−0.40 V, 25 °C) is very close to that of zerovalent iron (−0.41 V, 25 °C), and thus, the removal of Cd^{2+} ions by nZVI is due to sorption [21].

Although previous research has investigated adsorption and redox processes as the removal mechanisms of metals by nano iron, comparatively little research has investigated the detailed adsorption characteristics and thermodynamics of metal removal by nano iron [21–25,27]. Çelebi et al. [23] indicated that the adsorption of Ba^{2+} on nZVI particles follows pseudo-second-order kinetics and the Dubinin–Radushkevich isotherm can be used to model the adsorption process. The Freundlich equation was used to model Pb^{2+} adsorption on amino-functionalized nZVI particles [29]. The adsorption of As^{3+} and As^{5+} on carbon supported nZVI showed two distinct linear sorption stages and were modelled using the Langmuir and Freundlich isotherms [27]. To our knowledge cadmium

* Corresponding author. Tel.: +1 519 661 2111x88618; fax: +1 519 661 3779.
E-mail address: hboparai@uwo.ca (H.K. Boparai).

0304-3894/$ – see front matter © 2010 Elsevier B.V. All rights reserved.
doi:10.1016/j.jhazmat.2010.11.029

sorption onto nZVI particles has not been the subject of detailed study.

The objective of this research is to investigate the adsorption kinetics and isotherm models of cadmium removal by nano zerovalent iron at varying temperatures. Sorption kinetics is investigated to develop an understanding of controlling reaction pathways (e.g., chemisorption versus physisorption) and the mechanisms (e.g., surface versus intraparticle diffusion) of sorption reactions. Kinetic data can be used to predict the rate at which the target contaminant is removed from aqueous solutions and equilibrium adsorption isotherms are used to quantify the adsorptive capacity of an adsorbent (e.g., nZVI). Results from this study can be used to assess the utility of nZVI for heavy metal removal, in particular cadmium adsorption, at the field scale.

2. Materials and methods

2.1. Preparation of nZVI

nZVI particles were synthesized using the 'bottom-up' method of dropwise addition of 0.125 M $NaBH_4$ aqueous solution to 0.023 M $FeCl_3$ solution with continuous stirring. Ferric iron (Fe^{3+}) was reduced to zerovalent iron (Fe^0) by borohydride according to the following reaction:

$$4Fe^{3+} + 3BH_4{}^- + 9H_2O \rightarrow 4Fe^0 \downarrow + 3H_2BO_3{}^- + 12H^+ + 6H_2 \uparrow \quad (1)$$

Black nZVI particles appeared immediately after introducing the first few drops of $NaBH_4$ solution. After the addition of $NaBH_4$ solution, the mixture was stirred for an additional 20 min. nZVI particles were collected and washed thrice with iso-propanol to prevent oxidation. Deionized deoxygenated water (sparged with nitrogen) was used to prepare aqueous solutions. nZVI synthesis was conducted in an anaerobic chamber maintaining an O_2-free environment by purging with O_2-free Ar (95% Ar:5% H_2).

2.2. Adsorption experiments

To study the temperature effect on the kinetics of Cd^{2+} adsorption by nZVI, 0.5 g L^{-1} nZVI was added to each glass vial containing 60 mL of 112.5 mg L^{-1} Cd^{2+} solution. The glass vials were capped with Teflon Mininert valves to minimize oxidation of nZVI particles during the equilibration period. Experiments were carried out at five temperatures (285, 297, 307, 313 and 333 K) by placing the glass vials on a temperature controlled shaker. Samples were collected at 0, 1, 3, 5, 8, 12, 24, 48, and 72 h for Cd^{2+} analysis. Independent blank experiments (i.e., no nZVI) found that there was no Cd^{2+} adsorption to the glass vials and valves.

Adsorption isotherms were obtained by varying the initial Cd^{2+} concentration from 25 to 450 mg L^{-1} in 60 mL vials with 0.5 g L^{-1} nZVI at three temperatures (285, 297 and 307 K). The samples were collected at 0 and 72 h to quantify initial and final Cd^{2+} concentrations. All experiments were performed in duplicate inside the anaerobic chamber.

Sample aliquots collected were filtered with 0.2 μm syringe filters. The filtrates were diluted with nitric acid and Cd^{2+} concentrations determined by ICP-OES.

2.3. SEM/EDX and BET analyses

The surface morphology of nZVI was characterized by Scanning Electron Microscope (SEM, Hitachi S-2600N, 5.0 kV). The solid samples were sprinkled onto adhesive carbon tape supported on metallic disks. The elemental composition of nZVI before and after cadmium adsorption was determined by randomly selecting areas on the solid surfaces and analyzing by energy dispersive X-ray (EDX) in conjunction with SEM. The specific surface area of nZVI particles was measured by Burnauer–Emmett–Teller (BET) N_2 method using a Micrometrics ASAP 2010 BET surface area analyzer.

3. Theory

3.1. Adsorption kinetics

Metal uptake q (mg metal ion per g nZVI) was determined by mass balance, as follows [8]:

$$q_t = (C_0 - C_t) \times \frac{V}{m} \quad (2)$$

where C_0 and C_t are cadmium concentrations (mg L^{-1}) at time 0 and t, respectively, V is the volume of the solution (mL), and m is the mass of nZVI (g).

Parameters from two kinetic models, pseudo first-order [30,31] and pseudo second-order [31,32], were fit to experimental data to examine the adsorption kinetics of cadmium uptake by nZVI.

3.1.1. Pseudo first-order kinetics

The pseudo first-order equation (Lagergren's equation) describes adsorption in solid–liquid systems based on the sorption capacity of solids [30]. It is assumed that one cadmium ion is sorbed onto one sorption site on the nZVI surface:

$$A + Cd^{2+}_{aq} \xrightarrow{k_1} ACd_{\text{solid phase}} \quad (3)$$

where A represents an unoccupied sorption site on the nZVI and k_1 is the pseudo first order rate constant (h^{-1}).

The linear form of pseudo first order model can be expressed as:

$$\log(q_e - q_t) = \log q_e - \frac{k_1}{2.303} t \quad (4)$$

where q_e and q_t (mg g^{-1}) are the adsorption capacities at equilibrium and at time t (h), respectively.

3.1.2. Pseudo-second order kinetics

The pseudo second-order rate expression, which has been applied for analyzing chemisorption kinetics from liquid solutions [31,32], is linearly expressed as:

$$\frac{t}{q_t} = \frac{1}{k_2 {q_e}^2} + \frac{1}{q_e} t \quad (5)$$

where k_2 is the rate constant for pseudo second-order adsorption (g mg^{-1} h^{-1}) and $k_2 {q_e}^2$ or h (mg g^{-1} h^{-1}) is the initial adsorption rate.

This model assumes that one cadmium ion is sorbed onto two sorption sites on the nZVI surface:

$$2A + Cd^{2+}_{sol} \xrightarrow{k_2} A_2Cd_{\text{solid phase}} \quad (6)$$

3.1.3. Goodness of adsorption kinetic model fit

The best fit among the kinetic models is assessed by the linear coefficient of determination (r^2) and non-linear Chi-square (χ^2).

The Chi-square test measures the difference between the experimental and model data. The mathematical form of this test statistic can be expressed as:

$$\chi^2 = \sum \frac{(q_{e,\text{exp}} - q_{e,\text{cal}})^2}{q_{e,\text{cal}}} \quad (7)$$

where $q_{e,\text{exp}}$ is experimental equilibrium capacity data and $q_{e,\text{cal}}$ is the equilibrium capacity from a model. If data from the model are similar to experimental data, χ^2 will be small and if they differ, χ^2 will be large.

3.2. The Arrhenius equation

The Arrhenius equation for calculating adsorption activation energy is expressed as:

$$k_2 = k \exp\left(-\frac{E_a}{RT}\right) \quad (8)$$

where k is the temperature-independent factor ($g\,mg^{-1}\,h^{-1}$), E_a the activation energy of sorption ($kJ\,mol^{-1}$), R the universal gas constant ($8.314\,J\,mol^{-1}\,K$) and T the solution temperature (K).

3.3. Intraparticle diffusion equation

The intraparticle diffusion equation is expressed as:

$$q_t = k_i t^{0.5} + C \quad (9)$$

where k_i is the intraparticle diffusion rate constant ($mg\,g^{-1}\,min^{0.5}$) and C is the intercept.

3.4. Adsorption isotherm models

An adsorption isotherm describes the fraction of sorbate molecules that are partitioned between liquid and solid phases at equilibrium. Adsorption of Cd^{2+} ions by nZVI particles was modelled using four adsorption isotherms.

3.4.1. Freundlich isotherm

The Freundlich isotherm is applicable to both monolayer (chemisorption) and multilayer adsorption (physisorption) and is based on the assumption that the adsorbate adsorbs onto the heterogeneous surface of an adsorbent [33]. The linear form of Freundlich equation is expressed as:

$$\log q_e = \log K_F + \frac{1}{n}\log C_e \quad (10)$$

where K_F and n are Freundlich isotherm constants related to adsorption capacity and adsorption intensity, respectively and C_e is the equilibrium concentration ($mg\,L^{-1}$) [7].

3.4.2. Langmuir isotherm

The Langmuir isotherm assumes monolayer adsorption on a uniform surface with a finite number of adsorption sites. Once a site is filled, no further sorption can take place at that site. As such the surface will eventually reach a saturation point where the maximum adsorption of the surface will be achieved. The linear form of the Langmuir isotherm model is described as:

$$\frac{C_e}{q_e} = \frac{1}{K_L q_m} + \frac{C_e}{q_m} \quad (11)$$

where K_L is the Langmuir constant related to the energy of adsorption and q_m is the maximum adsorption capacity ($mg\,g^{-1}$) [7,34,35].

3.4.3. Temkin isotherm

The Temkin isotherm model assumes that the adsorption energy decreases linearly with the surface coverage due to adsorbent–adsorbate interactions. The linear form of Temkin isotherm model is given by the equation:

$$q_e = \frac{Rt}{b}\ln K_T + \frac{RT}{b}\ln C_e \quad (12)$$

where b is the Temkin constant related to the heat of sorption ($J\,mol^{-1}$) and K_T is the Temkin isotherm constant ($L\,g^{-1}$) [23].

3.4.4. Dubinin–Radushkevich (D–R) isotherm

The D–R isotherm model is a semi-empirical equation where adsorption follows a pore filling mechanism. It assumes that the adsorption has a multilayer character, involves van der Waals forces and is applicable for physical adsorption processes [36]. The linear form of D–R isotherm model is expressed as:

$$\ln q_e = \ln q_d - \beta\varepsilon^2 \quad (13)$$

where q_d is the D–R constant ($mg\,g^{-1}$), β is the constant related to free energy and ε is the Polanyi potential which is defined as:

$$\varepsilon = RT\ln\left[1+\frac{1}{C_e}\right] \quad (14)$$

3.5. Thermodynamic parameters

The thermodynamic parameters can be determined from the thermodynamic equilibrium constant, K_0 (or the thermodynamic distribution coefficient). The standard Gibbs free energy ΔG^o ($kJ\,mol^{-1}$), standard enthalpy change ΔH^o ($kJ\,mol^{-1}$), and standard entropy change ΔS^o ($J\,mol^{-1}\,K^{-1}$) were calculated using the following equations:

$$\Delta G^o = -RT\ln K_0 \quad (15)$$

$$\ln K_0 = \frac{\Delta S^o}{R} - \frac{\Delta H^o}{RT} \quad (16)$$

K_0 can be defined as:

$$K_0 = \frac{a_s}{a_e} = \frac{\gamma_s}{\gamma_e}\frac{C_s}{C_e} \quad (17)$$

where a_s = activity of adsorbed Cd^{2+}, a_e = activity of Cd^{2+} in solution at equilibrium, γ_s = activity coefficient of adsorbed Cd^{2+}, γ_e = activity coefficient of Cd^{2+} in equilibrium solution, C_s = Cd^{2+} adsorbed on nZVI ($mmol\,g^{-1}$), and C_e = Cd^{2+} concentration in equilibrium solution ($mmol\,mL^{-1}$).

The expression of K_0 can be simplified by assuming that the concentration in the solution approaches zero resulting in $C_s \to 0$ and $C_e \to 0$ and the activity coefficients approach unity at these very low concentrations [37,38]. Eq. (16) can be written as:

$$C_s \xrightarrow{\lim} 0 \frac{C_s}{C_e} = \frac{a_s}{a_e} = K_0 \quad (18)$$

4. Results and discussion

4.1. Adsorption kinetics

Temperature is an important factor governing the sorption process. The effect of temperature on the adsorption of cadmium by nano zerovalent iron was studied from 285 to 333 K at $C_0 = 112\,mg\,L^{-1}$ and an nZVI loading = $0.5\,g\,L^{-1}$. An increase in the temperature resulted in increasing cadmium adsorption rate indicating the process to be endothermic (Fig. 1). This will be further discussed in relation to thermodynamic parameters in Section 4.5. Similar trend has been reported for the removal of arsenate by nanosized modified zerovalent iron in a similar temperature range [25]. The time required to reach sorption equilibrium is 12 h at temperatures ranging between 307 and 333 K, 24 h at 297 K and 48 h at 285 K. This may be due to the higher rate of diffusion of Cd^{2+} ions onto the nZVI particle surface at higher temperatures [39]. The equilibrium cadmium adsorption was however relatively insensitive to temperature, increasing from $213\,mg\,g^{-1}$ at 285 K to $225\,mg\,g^{-1}$ at 333 K (Table 1).

To evaluate the kinetics of the adsorption process, the pseudo first-order and pseudo second-order models were tested to interpret the experimental data.

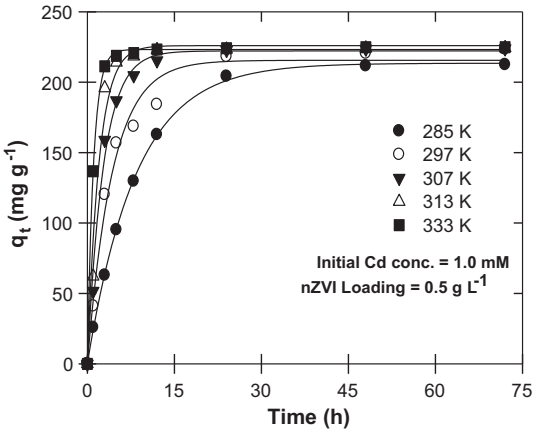

Fig. 1. Effect of temperature on the sorption kinetics of cadmium by nZVI particles.

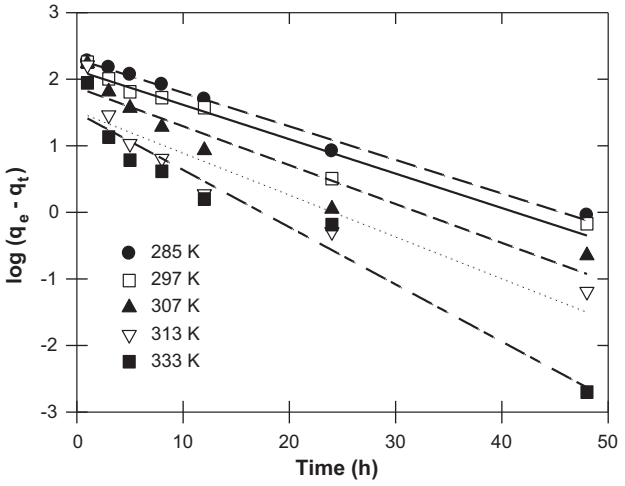

Fig. 2. Pseudo first-order kinetic model fit for Cd^{2+} sorption onto nZVI particles at various temperatures.

4.1.1. Pseudo first-order kinetics

k_1 and q_e, at the temperatures evaluated experimentally, were calculated using the slope and intercept of plots of $\log(q_e - q_t)$ versus t (Fig. 2, Table 1). Best fit lines at each temperature yielded relatively high $r_1{}^2$ values however close inspection of the model fit and experimental observations in Fig. 2 suggest that application of Eq. (4) is inappropriate as experimental observations are non-linear when plotted in this manner. In addition agreement between experimentally observed equilibrium adsorption and that derived using Eq. (4) is poor (Table 1). This suggests that the adsorption of cadmium on nZVI did not follow pseudo first-order kinetics.

4.1.2. Pseudo-second order kinetics

Pseudo second-order adsorption parameters $q_{e,cal}$ and k_2 in Eq. (5) were determined by plotting t/qt versus t (Fig. 3, Table 1). Fitted equilibrium adsorption capacities derived from Eq. (5) are similar

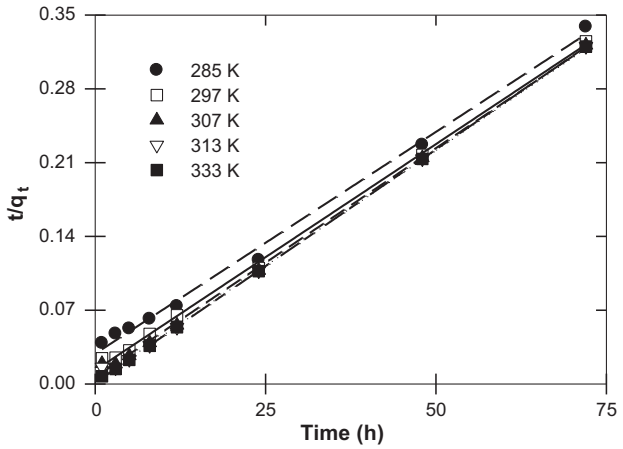

Fig. 3. Pseudo second-order kinetics of Cd^{2+} sorption onto nZVI particles at various temperatures.

at each temperature and in close agreement with those observed experimentally. Furthermore the correlation coefficients ($r_2{}^2$) for the pseudo second-order kinetic model fits are 1.00, much higher than the correlation coefficients derived from pseudo first-order model fits. Given the good agreement between model fit and experimentally observed equilibrium adsorption capacity in addition to the large correlation coefficients, this suggests that cadmium adsorption followed pseudo second-order kinetics and Cd^{2+} ions were adsorbed onto the nZVI surface via chemical interaction. Similar trends have been reported for the adsorption of Cd^{2+} ions from aqueous solutions by other adsorbents [4,8,11].

The lower χ^2 value of 3.72 for the pseudo-second order model also suggests that Cd^{2+} adsorption onto nZVI particles followed the pseudo-second order kinetics. The pseudo-first order model exhibited higher χ^2 values (2682) suggesting poor pseudo-first order fit to the data for cadmium adsorption on nZVI.

4.2. Adsorption activation energy

Cd^{2+} adsorption rate constants were determined at a number of temperatures from experimental data assuming pseudo second-order kinetics. Arrhenius equation parameters are fitted using these rate constants to determine temperature independent rate parameters and adsorption type. A plot of $\ln k_2$ versus $1/T$ yields a straight line, with slope $-E_a/R$ (Fig. 4). The magnitude of the activation energy is commonly used as the basis for differentiating between physical and chemical adsorption. Physical adsorption reactions are readily reversible, equilibrium attained rapidly and thus energy requirements are small, ranging from 5 to 40 kJ mol^{-1}. Chemical adsorption is specific, involves stronger forces and thus requires larger activation energies (e.g., 40–800 kJ mol^{-1}) [40,41]. The activation energy for Cd^{2+} adsorption onto nZVI was 54.8 kJ mol^{-1} suggesting that the Cd^{2+} ions was chemically adsorbed onto the nZVI surface.

Table 1
Adsorption kinetic model rate constants for Cd^{2+} adsorption on nZVI particles at different temperatures.

Temperature (K)	$q_{e,exp}$ (mg g^{-1})	Pseudo first-order			Pseudo second-order			
		k_1 (h^{-1})	$q_{e,cal}$ (mg g^{-1})	$r_1{}^2$	$k_2 \times 10^{-3}$ (g mg^{-1} h^{-1})	$q_{e,cal}$ (mg g^{-1})	h (mg g^{-1} h^{-1})	$r_2{}^2$
285	213	0.1163	200	0.99	0.61	238	34.8	1.00
297	222	0.1191	136	0.95	1.42	233	76.9	1.00
307	224	0.1345	75	0.92	2.89	233	156.3	1.00
313	225	0.1449	33	0.86	5.38	227	277.8	1.00
333	225	0.1981	31	0.95	16.10	227	833.3	1.00

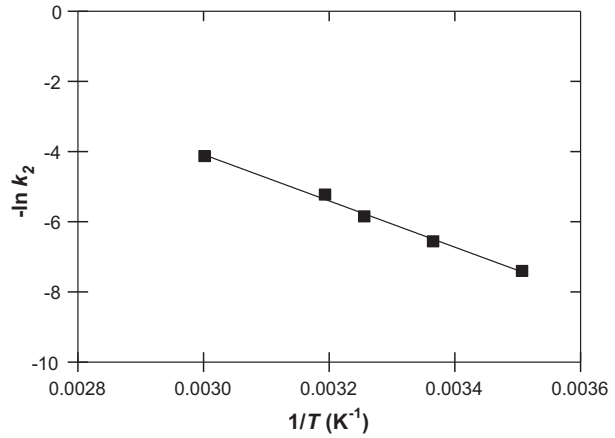

Fig. 4. Determination of the activation energy for Cd^{2+} adsorption on nZVI particles.

4.3. Adsorption mechanisms

A detailed understanding of adsorption mechanisms facilitates a determination of the rate-limiting step. This information can then be used to optimize the design of adsorbents and adsorption conditions. The overall rate of adsorption can be described by the following three steps [35]: (1) film or surface diffusion where the sorbate is transported from the bulk solution to the external surface of sorbent, (2) intraparticle or pore diffusion, where sorbate molecules move into the interior of sorbent particles, and (3) adsorption on the interior sites of the sorbent. Since the adsorption step is very rapid, it is assumed that it does not influence the overall kinetics. The overall rate of adsorption process, therefore, will be controlled by either surface diffusion or intraparticle diffusion. The Weber–Morris intraparticle diffusion model has often been used to determine if intraparticle diffusion is the rate-limiting step [42–44].

According to this model, a plot of q_t versus $t^{0.5}$ should be linear if intraparticle diffusion is involved in the adsorption process and if the plot passes through the origin then intraparticle diffusion is the sole rate-limiting step [41]. It has also been suggested that in instances when q_t versus $t^{0.5}$ is multilinear two or more steps govern the adsorption process [40,43]. Given the multilinearity of this plot for adsorption of Cd on nZVI particles, this suggests that adsorption occurred in three phases (Fig. 5). The initial steeper section represents surface or film diffusion, the second linear section represents a gradual adsorption stage where intraparticle or pore diffusion is rate-limiting and the third section is final equilibrium stage. As the plot did not pass through the origin, intraparticle diffusion was not the only rate-limiting step. Thus, there were three processes controlling the adsorption rate but only one was rate-limiting in any particular time range. The intraparticle diffusion rate constant k_i was calculated from the slope of the second linear section (Fig. 5, Table 2). The value of the intercept C in this second section provides information related to the thickness of the boundary layer [44]. Larger intercepts suggest that surface diffusion has a larger role as the rate-limiting step. The intercept values increased with the increasing temperature. This suggests that the surface diffusion became more important at high temperatures because of the greater random motion associated with the increased thermal energy [45].

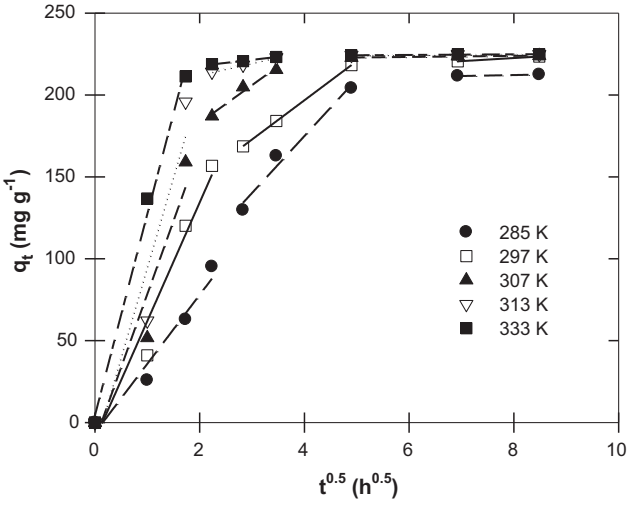

Fig. 5. Intraparticle diffusion plots for Cd^{2+} adsorption on nZVI at different temperatures.

Table 2
Intraparticle diffusion coefficients and intercept values for Cd^{2+} adsorption on nZVI particles at different temperatures.

Temperature (K)	K_i (mg g^{-1} $h^{0.5}$)	Intercept values (C)	r_i^2
285	34.76	35.85	0.98
297	23.93	101.1	1.00
307	22.90	137.1	0.97
313	7.21	198.0	1.00
333	3.68	210.4	1.00

4.4. Adsorption isotherms

Adsorption of Cd^{2+} ions by nZVI particles was modelled using the Freundlich, Langmuir, Temkin, and Dubinin–Radushkevich (D–R) isotherms with the quality of the fit assessed using the correlation coefficient.

The Freundlich isotherm constants K_F and n are determined from the intercept and slope of a plot of $\log q_e$ versus $\log C_e$ (Fig. 6A). In this study n values are greater than unity indicating chemisorption (Table 3) [46]. Isotherms with $n > 1$ are classified as L-type isotherms reflecting a high affinity between adsorbate and adsorbent and is indicative of chemisorption [47]. The Freundlich constant, K_F, which is related to the adsorption capacity, increased with temperature, indicating that the adsorption process is endothermic.

The slope and intercept of plots of C_e/q_e versus C_e, at different temperatures, were used to calculate q_m and K_L (Fig. 6B). Langmuir isotherm parameter fits (Table 3) for Cd^{2+} adsorption on nZVI yielded isotherms that were in good agreement with observed behaviour ($r_L^2 \geq 0.99$). The cadmium adsorption capacity on nZVI at room temperature (297 K) was 769.2 mg g^{-1} (Table 3). This is much higher than the adsorption capacity of other adsorbents reported in the literature: activated carbon (3.37 mg g^{-1}) [12], hematite (4.94 mg g^{-1}) [18], wheat stem (11.6 mg g^{-1}) [7], chitin (14.7 mg g^{-1}) [8], orange waste (48.3 mg g^{-1}) [4], bone char (64.1 mg g^{-1}) [48], activated sludge (204.1 mg g^{-1}) [11], and biogenic Mn oxides (229.3 mg g^{-1}) [9].

Linear plots for Temkin adsorption isotherm (Fig. 6C), which consider chemisorption of an adsorbate onto the adsorbent [49], fit quite well with correlation coefficients ≥0.97 (Table 3). This further supports the findings that the adsorption of cadmium onto nZVI particles is a chemisorption process.

The slope and intercept of plots of $\ln q_e$ versus ε^2, at different temperatures, were used to calculate the D–R isotherm parameters β and q_d (data not shown). The q_d values are not consistent with the q_m values previously determined for the Langmuir isotherm. The magnitude of the correlation coefficients for the D–R isotherm is the lowest when compared to the other three isotherm models (Table 3). This suggests that the cadmium adsorption onto nZVI particles is not a physical process.

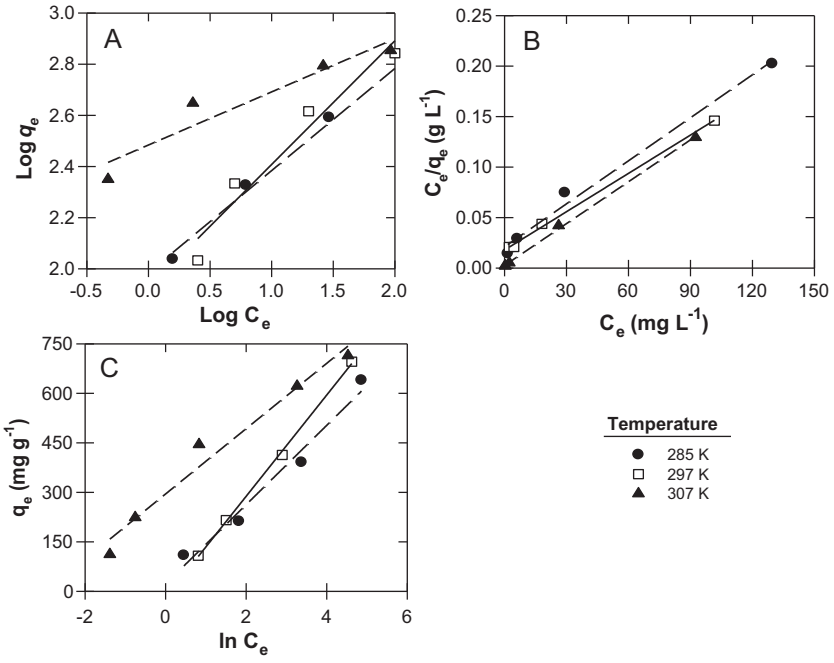

Fig. 6. Linearized (A) Freundlich, (B) Langmuir, and (C) Temkin isotherms for Cd^{2+} adsorption on nZVI particles at different temperatures.

Table 3
Langmuir, Freundlich, Temkin, and D–R isotherm model parameters and correlation coefficients for adsorption of cadmium on nZVI particles.

Isotherm	Temperature (K)	Parameters		r^2
		K_F	n	
Freundlich	285	96.7	2.50	0.99
	297	91.0	2.13	0.94
	307	305.0	4.76	0.91

Isotherm	Temperature (K)	Parameters		r^2
		q_m (mg g^{-1})	K_L (L mg^{-1})	
Langmuir	285	714.3	0.07	0.99
	297	769.2	0.07	1.00
	307	714.3	0.54	1.00

Isotherm	Temperature (K)	Parameters		r^2
		K_T	b	
Temkin	285	1.21	19.7	0.97
	297	0.89	16.1	1.00
	307	19.78	25.8	0.97

Isotherm	Temperature (K)	Parameters		r^2
		q_d	B_d	
D–R	285	399.1	0.71	0.73
	297	486.3	0.51	0.86
	307	473.4	3.18	0.85

4.5. Thermodynamic studies

An increase in temperature resulted in an increased rate of cadmium adsorption indicating that the process is endothermic (Fig. 1). Thermodynamic parameters for Cd^{2+} adsorption were quantified to increase the utility of measured data and fit parameters to a broader range of temperatures.

K_0 at different temperatures was determined by plotting $\ln(C_s/C_e)$ versus C_s (Fig. 7A) and extrapolating C_s to zero [37,38]. K_0 increased with temperature indicating that the adsorption was endothermic (Table 4). Negative values of ΔG^o indicate spontaneous adsorption and the degree of spontaneity of the reaction increases with increasing temperature. $\ln K_0$ was plotted against $1/T$ to calculate ΔH^o and ΔS^o from the slope and intercept, respectively (Fig. 7B) [50,51]. The positive standard enthalpy change of 7.17 kJ mol^{-1} for this study suggests that the adsorption of Cd^{2+} by nZVI is endothermic, which is supported by the increasing adsorp-

Table 4
Thermodynamic parameters for adsorption of cadmium onto nZVI particles.

Temperature (K)	K_0	ΔG^o (kJ mol^{-1})
285	11.6	−5.83
297	12.1	−6.18
307	14.5	−6.85

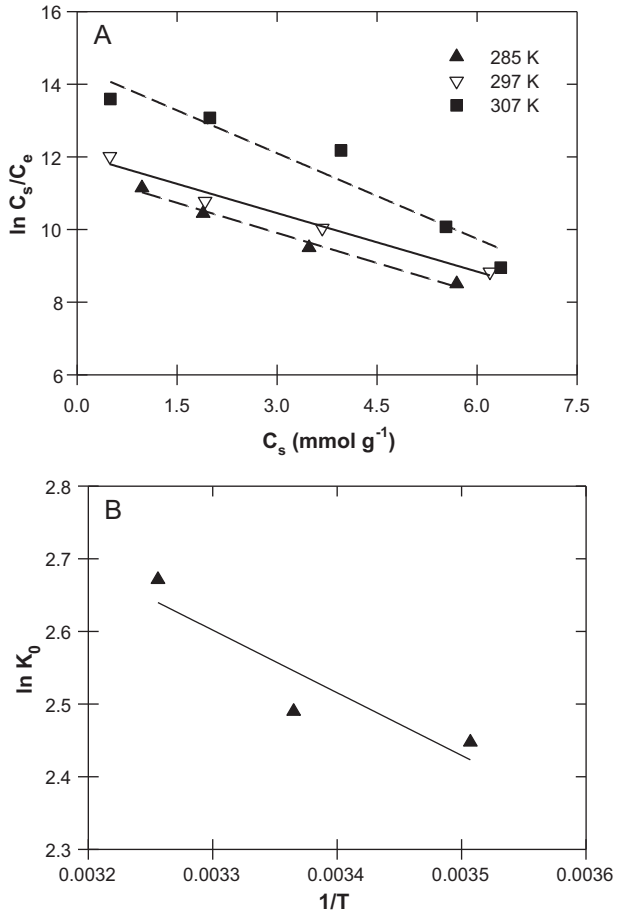

Fig. 7. (A) Plots of $\ln(C_s/C_e)$ versus C_s at various temperatures and (B) plot of K_0 versus $1/T$.

tion of Cd^{2+} with increase in temperature. The positive standard entropy change (45.3 J mol^{-1} K^{-1}) reflects the affinity of the nZVI particles towards Cd^{2+} [34].

4.6. SEM–EDX analysis

Adsorbent (i.e, nZVI) shape and size impact the adsorption capacity of the adsorbent. SEM images of fresh nZVI particles indicate that the material is composed of individual, spherical particles ranging in size from 20 to 200 nm that form aggregates and chains (Fig. 8). This small nZVI particle size provides a larger surface area for contaminant adsorption. The freshly prepared nZVI has a specific surface area of 26.3 m^2 g^{-1}, as measured by BET.

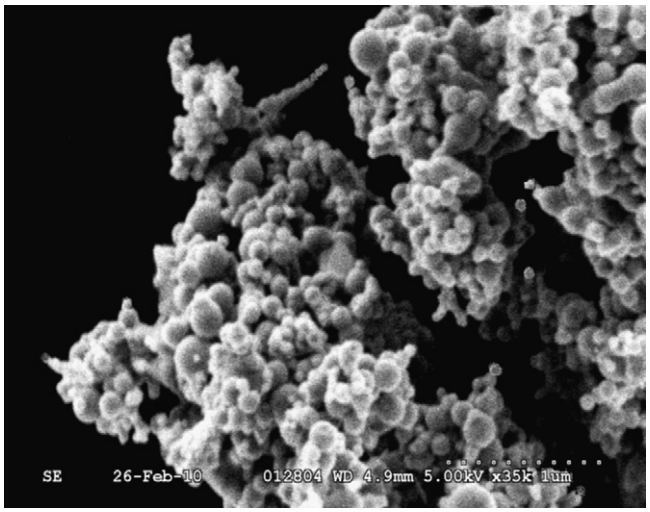

Fig. 8. SEM analysis of fresh nZVI particles.

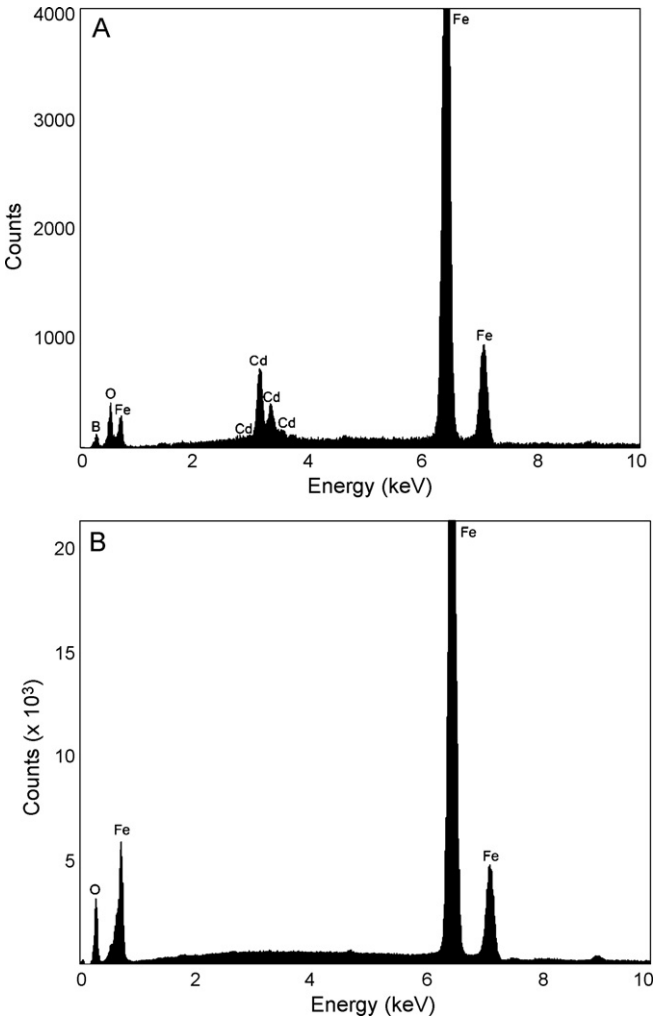

Fig. 9. Energy dispersive X-ray (EDX) analysis of nZVI particles (A) before and (B) after the adsorption of Cd^{2+} ions.

Energy dispersive X-ray (EDX) analysis was conducted to evaluate the adsorption of Cd^{2+} on nZVI particles. The EDX spectrum for fresh nZVI particles indicated the presence of Fe, O and B in the structure (Fig. 9A) but did not show the characteristic signal of Cd^{2+} ions on the surface of freshly synthesized nZVI. An EDX spectrum was also recorded for Cd^{2+}-adsorbed nZVI particles after exposing 2 g L^{-1} nZVI to an initial concentration of 450 mg L^{-1} Cd^{2+} (Fig. 9B). The EDX spectrum gives the characteristic peaks for Cd at 2.95, 3.20, 3.45 and 3.75 keV which is similar to the Cd^{2+} ion signals observed at the same energy in the Cd-loaded bamboo charcoal [17]. This confirms the binding of the cadmium ions to the nZVI surface.

5. Conclusions

Nano zerovalent iron can be used as an effective adsorbent for removing cadmium from contaminated water sources. Increasing the temperature increased the cadmium adsorption rate but the maximum adsorption capacity was similar. The pseudo second-order kinetic model accurately described the adsorption kinetics. The adsorption mechanism was found to be chemisorption and the rate-limiting step was mainly surface adsorption. The Langmuir

isotherm showed a better fit than the Freundlich isotherm, thus, indicating the applicability of monolayer coverage of cadmium on nZVI surface. The equilibrium data were also well described by the Temkin equation further supporting cadmium adsorption on nZVI as a chemisorption process. Thermodynamic analysis showed that the adsorption process was endothermic and spontaneous in nature. EDX analysis confirmed that Cd^{2+} was adsorbed onto the nZVI particles. Results from this study suggest that nZVI is a very effective adsorbent for cadmium, as anticipated.

Acknowledgements

This research was supported by the EJLB Foundation, Ontario Centres of Excellence and Canadian Foundation for Innovation Grant.

References

[1] M.P. Waalkes, Cadmium carcinogenesis in review, J. Inorg. Biochem. 79 (2000) 241–244.
[2] Y.C. Sharma, Thermodynamics of removal of cadmium by adsorption on an indigenous clay, Chem. Eng. J. 145 (2008) 64–68.
[3] B.J. Alloway, E. Steinnes, Anthropogenic additions of cadmium to soils, in: M.J. McLaughlin, B.R. Singh (Eds.), Cadmium in Soils and Plants, Kluwer Academic Publishers, Boston, 1999, pp. 97–124.
[4] A.B. Perez-Marin, V.M. Zapata, J.F. Ortuno, M. Aguilar, J. Saez, M. Llorens, Removal of cadmium from aqueous solutions by adsorption onto orange waste, J. Hazard. Mater. 139 (2007) 122–131.
[5] M.P. Mahalik, H.W. Hitner, W.C. Prozialeck, Teratogenic effects and distribution of cadmium (Cd^{2+}) administered via osmotic minipumps to gravid Cf-1 mice, Toxicol. Lett. 76 (1995) 195–202.
[6] WHO, Guidelines for Drinking Water Quality: Recommendations, vol. 1, 3rd ed., World Health Organisation, Geneva, 2008.
[7] G.Q. Tan, D. Xiao, Adsorption of cadmium ion from aqueous solution by ground wheat stems, J. Hazard. Mater. 164 (2009) 1359–1363.
[8] B. Benguella, H. Benaissa, Cadmium removal from aqueous solutions by chitin: kinetic and equilibrium studies, Water Res. 36 (2002) 2463–2474.
[9] Y.T. Meng, Y.M. Zheng, L.M. Zhang, J.Z. He, Biogenic Mn oxides for effective adsorption of Cd from aquatic environment, Environ. Pollut. 157 (2009) 2577–2583.
[10] N. Cihangir, N. Saglam, Removal of cadmium by Pleurotus sajor-caju basidiomycetes, Acta Biotechnol. 19 (1999) 171–177.
[11] R.D.C. Soltani, A.J. Jafari, Gh.S. Khorramabadi, Investigation of cadmium (II) ions biosorption onto pretreated dried activated sludge, Am. J. Environ. Sci. 5 (2009) 41–46.
[12] H.K. An, B.Y. Park, D.S. Kim, Crab shell for the removal of heavy metals from aqueous solution, Water Res. 35 (2001) 3551–3556.
[13] R. Cortes-Martinez, V. Martinez-Miranda, M. Solache-Rios, I. Garcia-Sosa, Evaluation of natural and surfactant-modified zeolites in the removal of cadmium from aqueous solutions, Sep. Sci. Technol. 39 (2004) 2711–2730.
[14] U. Garg, M.P. Kaur, G.K. Jawa, D. Sud, V.K. Garg, Removal of cadmium (II) from aqueous solutions by adsorption on agricultural waste biomass, J. Hazard. Mater. 154 (2008) 1149–1157.
[15] L. Semerjian, Equilibrium and kinetics of cadmium adsorption from aqueous solutions using untreated *Pinus halepensis* sawdust, J. Hazard. Mater. 173 (2010) 236–242.
[16] Z.Z. Li, T. Katsumi, S. Imaizumi, X.W. Tang, T. Inui, Cd(II) adsorption on various adsorbents obtained from charred biomaterials, J. Hazard. Mater. 183 (2010) 410–420.
[17] F.Y. Wang, H. Wang, J.W. Ma, Adsorption of cadmium (II) ions from aqueous solution by a new low-cost adsorbent-Bamboo charcoal, J. Hazard. Mater. 177 (2010) 300–306.
[18] D.B. Singh, D.C. Rupainwar, G. Prasad, K.C. Jayaprakas, Studies on the Cd(II) removal from water by adsorption, J. Hazard. Mater. 60 (1998) 29–40.
[19] H.R. Tashauoei, H.M. Attar, M.M. Amin, M. Kamali, M. Nikaeen, M.V. Dastjerdi, Removal of cadmium and humic acid from aqueous solutions using surface modified nanozeolite A, Int. J. Environ. Sci. Technol. 7 (2010) 497–508.
[20] M. Visa, C. Bogatu, A. Duta, Simultaneous adsorption of dyes and heavy metals from multicomponent solutions using fly ash, Appl. Surf. Sci. 256 (2010) 5486–5491.
[21] X.Q. Li, W.X. Zhang, Sequestration of metal cations with zerovalent iron nanoparticles—a study with high resolution X-ray photoelectron spectroscopy (HR-XPS), J. Phys. Chem. C 111 (2007) 6939–6946.
[22] C. Uzum, T. Shahwan, A.E. Eroglu, K.R. Hallam, T.B. Scott, I. Lieberwirth, Synthesis and characterization of kaolinite-supported zero-valent iron nanoparticles and their application for the removal of aqueous Cu^{2+} and Co^{2+} ions, Appl. Clay Sci. 43 (2009) 172–181.
[23] O. Çelebi, C. Uzum, T. Shahwan, H.N. Erten, A radiotracer study of the adsorption behavior of aqueous Ba^{2+} ions on nanoparticles of zero-valent iron, J. Hazard. Mater. 148 (2007) 761–767.
[24] S.R. Kanel, B. Manning, L. Charlet, H. Choi, Removal of arsenic(III) from groundwater by nanoscale zero-valent iron, Environ. Sci. Technol. 39 (2005) 1291–1298.
[25] G. Jegadeesan, K. Mondal, S.B. Lalvani, Arsenate remediation using nanosized modified zerovalent iron particles, Environ. Prog. 24 (2005) 289–296.
[26] J.T. Nurmi, P.G. Tratnyek, V. Sarathy, D.R. Baer, J.E. Amonette, K. Pecher, C.M. Wang, J.C. Linehan, D.W. Matson, R.L. Penn, M.D. Driessen, Characterization and properties of metallic iron nanoparticles: spectroscopy, electrochemistry, and kinetics, Environ. Sci. Technol. 39 (2005) 1221–1230.
[27] H. Zhu, Y. Jia, X. Wu, H. Wang, Removal of arsenic from water by supported nano zero-valent iron on activated carbon, J. Hazard. Mater. 172 (2009) 1591–1596.
[28] C.T. Yavuz, J.T. Mayo, W.W. Yu, A. Prakash, J.C. Falkner, S. Yean, L.L. Cong, H.J. Shipley, A. Kan, M. Tomson, D. Natelson, V.L. Colvin, Low-field magnetic separation of monodisperse Fe_3O_4 nanocrystals, Science 314 (2006) 964–967.
[29] Q.Y. Liu, Y.L. Bei, F. Zhou, Removal of lead(II) from aqueous solution with amino-functionalized nanoscale zero-valent iron, Cent. Eur. J. Chem. 7 (2009) 79–82.
[30] Y.S. Ho, Citation review of Lagergren kinetic rate equation on adsorption reactions, Scientometrics 59 (2004) 171–177.
[31] Y.S. Ho, Review of second-order models for adsorption systems, J. Hazard. Mater. 136 (2006) 681–689.
[32] S. Azizian, Kinetic models of sorption: a theoretical analysis, J. Colloid Interface Sci. 276 (2004) 47–52.
[33] C.H. Yang, Statistical mechanical study on the Freundlich isotherm equation, J. Colloid Interface Sci. 208 (1998) 379–387.
[34] M. Barkat, D. Nibou, S. Chearouche, A. Mellah, Kinetics and thermodynamics studies of chromium(VI) ions adsorption onto activated carbon from aqueous solutions, Chem. Eng. Process. 48 (2009) 38–47.
[35] P. Chingombe, B. Saha, R.J. Wakeman, Sorption of atrazine on conventional and surface modified activated carbons, J. Colloid Interface Sci. 302 (2006) 408–416.
[36] N.D. Hutson, R.T. Yang, Theoretical basis for the Dubinin–Radushkevitch (D–R) adsorption isotherm equation, Adsorption 3 (1997) 189–195.
[37] R. Calvet, Adsorption of organic-chemicals in soils, Environ. Health Persp. 83 (1989) 145–177.
[38] J.W. Biggar, M.W. Cheung, Adsorption of picloram (4-amino-3,5,6-trichloropicolinic acid) on Panoche, Ephrata, and Palouse soils—thermodynamic approach to adsorption mechanism, Soil Sci. Soc. Am. J. 37 (1973) 863–868.
[39] Y. Yu, Y.Y. Zhuang, Z.H. Wang, Adsorption of water-soluble dye onto functionalized resin, J. Colloid Interface Sci. 242 (2001) 288–293.
[40] E.I. Unuabonah, K.O. Adebowale, B.I. Olu-Owolabi, Kinetic and thermodynamic studies of the adsorption of lead (II) ions onto phosphate-modified kaolinite clay, J. Hazard. Mater. 144 (2007) 386–395.
[41] A. Ozcan, A.S. Ozcan, O. Gok, Adsorption kinetics and isotherms of anionic dye of reactive blue 19 from aqueous solutions onto DTMA-sepiolite, in: A.A. Lewinsky (Ed.), Hazardous Materials and Wastewater—Treatment, Removal and Analysis, Nova Science Publishers, New York, 2007.
[42] S.I.H. Taqvi, S.M. Hasany, M.Q. Bhanger, Sorption profile of Cd(II) ions onto beach sand from aqueous solutions, J. Hazard. Mater. 141 (2007) 37–44.
[43] F.C. Wu, R.L. Tseng, R.S. Juang, Initial behavior of intraparticle diffusion model used in the description of adsorption kinetics, Chem. Eng. J. 153 (2009) 1–8.
[44] D. Kavitha, C. Namasivayam, Experimental and kinetic studies on methylene blue adsorption by coir pith carbon, Bioresour. Technol. 98 (2007) 14–21.
[45] T.I. Kamins, Polycrystalline Silicon for Integrated Circuits and Displays, Kluwer Academic Publishers, Norwell, MA, 1998.
[46] J.Q. Jiang, C. Cooper, S. Ouki, Comparison of modified montmorillonite adsorbents—part I: preparation, characterization and phenol adsorption, Chemosphere 47 (2002) 711–716.
[47] M.R. Taha, K. Ahmad, A.A. Aziz, Z. Chik, Geoenvironmental aspects of tropical residual soils, in: B.B.K. Huat, G.S. Sew, F.H. Ali (Eds.), Tropical Residual Soils Engineering, A.A. Balkema Publishers, London, UK, 2009, pp. 377–403.
[48] C.W. Cheung, J.F. Porter, G. McKay, Sorption kinetic analysis for the removal of cadmium ions from effluents using bone char, Water Res. 35 (2001) 605–612.
[49] K. Biswas, S.K. Saha, U.C. Ghosh, Adsorption of fluoride from aqueous solution by a synthetic iron(III)–aluminum(III) mixed oxide, Ind. Eng. Chem. Res. 46 (2007) 5346–5356.
[50] F. Adam, J.H. Chua, The adsorption of palmytic acid on rice husk ash chemically modified with Al(III) ion using the sol–gel technique, J. Colloid Interface Sci. 280 (2004) 55–61.
[51] C. Raji, T.S. Anirudhan, Batch Cr(VI) removal by polyacrylamide-grafted sawdust: kinetics and thermodynamics, Water Res. 32 (1998) 3772–3780.